2nd International Symposium on Magnetic Beaing
July 12-14, 1990, Tokyo, Japan

H^∞ Robust Control Design for a Magnetic Suspension System

Masayuki Fujita, Fumio Matsumura, and Masanao Shimizu

Department of Electrical and Computer Engineering, Kanazawa University,
Kodatsuno 2-40-20, Kanazawa 920, Japan

Abstract: This paper presents an H^∞ robust control design for a magnetic suspension system with a flexible beam. The experimental apparatus utilized in this study is a simplified model of a magnetic bearing with a flexible rotor. Firstly, we describe the apparatus and formulate the mathematical model. Secondly, we set up an H^∞ control problem as the mixed sensitivity problem where the augmented plant is constructed with frequency weighting functions. The iterative computing environment MATLAB is then employed to calculate the controller. Thirdly, the controller is implemented using a digital signal processor NEC μPD77230 with 12-bit A/D and D/A converters. Finally, some experiments are carried out in order to evaluate the robustness of the H^∞ design. These experimental results show that the magnetic suspension system is robustly stable against various parameter changes and uncertainties.

1. Introduction

Magnetic bearings are bearings where the suspension forces are generated magnetically without any contact [1]. The structure of a magnetic bearing is shown schematically in Fig. 1. Several pairs of electromagnets are arranged radially around a rotor. By utilizing the magnetical forces of the electromagnets, we can support the rotor without any contact. It should be noted that these forces have to be controlled according to the motion of the rotor, since it is unstable in nature. Modeling and control of a magnetic bearing with its rigid body motion have been reported elsewhere (see, e.g., [2] - [8]). In case of high speed rotation, however, the rotor should be treated as a flexible one due to the effect of the deflection of the shaft. Now the control of magnetic bearings with a flexible rotor becomes more and more an important issue. In this paper, as a simplified model of an elastic rotor in a magnetic bearing, a magnetic suspension system with a flexible beam is fully utilized [9]. Further, in order to achieve robust stabilization, we try to apply the H^∞ control theory.

Recently the state-space formulae for the H^∞ control has been found (see [10],[11], and the references therein). The formulae involve the stabilizing solutions to two indefinite algebraic Riccati equations, which have the same form as those arising in the linear quadratic differential games [11],[12]. A direct consequence of the above results is that the associated complexity of computation is fairly reduced. Further, there has been a substantial development in the computer aided control systems design packages, such as Robust-Control Toolbox with MATLAB [13]. Accordingly, we could readily practice this powerful control methodology. Note that, despite voluminous publications on its theory, there have been few experimental evaluations for the performance of the H^∞ controller. Hence an application oriented study of the H^∞ control is also an challenging issue.

This paper presents an H^∞ robust control design for a magnetic suspension system with a flexible beam. In Section 2, we describe the experimental apparatus and formulate the mathematical model. In the apparatus, we intend to emphasize the first vibrational mode of the flexible beam. Section 3 is devoted to the control problem setup and the design of a controller. We set up an H^∞ control problem as the mixed sensitivity problem where the augmented plant is constructed with frequency weighting functions. The iterative computing environment MATLAB is then employed to calculate the controller. In Section 4, the controller is implemented using a digital signal processor NEC μPD77230 with 12-bit A/D and D/A converters. Several experiments are carried out in order to evaluate the robustness of the H^∞ design. These experimental results show that the magnetic suspension system is robustly stable against various parameter changes and uncertainties.

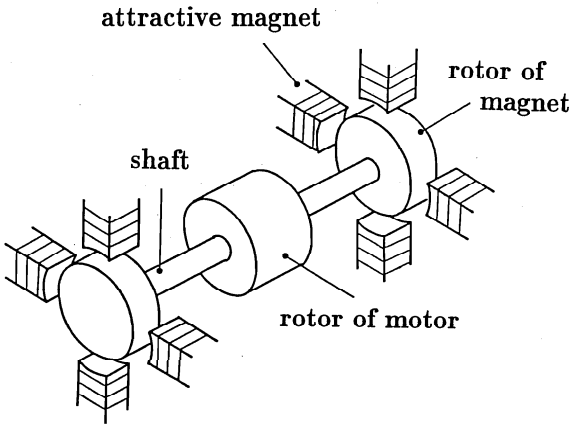

Fig. 1. Schematic diagram of magnetic bearing.

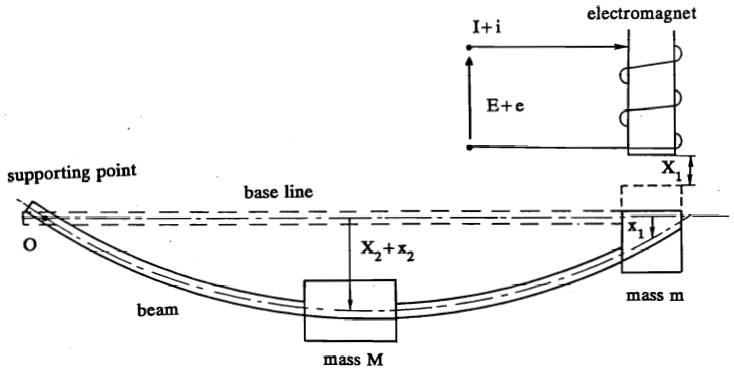

Fig. 2. Magnetic suspension system.

Table 1. Parameters.

parameter	symbols	values	units
beam length	2l	3.8	m
first order resonance frequency	f_n	4.5	Hz
deflection of the beam	X_2	12.3×10^{-3}	m
mass m	m	5.8	kg
mass M	M	10.36	kg
stationary gap of the electromagnet	X_1	5.0×10^{-3}	m
steady state current of the electromagnet	I	0.885	A
resistance of the electromagnet	R	57	Ω
inductance of the electromagnet	L	3.16	H

2. System Description and Modeling

2.1. Description of Apparatus

As a simplified model of a magnetic bearing for a flexible rotor, we consider a magnetic suspension system with a flexible beam shown in Fig. 2 [9]. The experimental configuration which is fully utilized throughout the paper, consists of a flexible aluminum beam with a electromagnet and a gap sensor. The beam is supported by a hinge at the left side and it will be suspended stably by the force of the electromagnet at the right side. The beam is reasonably stiff in torsion bending and is free to rotate at the supporting point O. Thus it can be assumed that the motion of the beam is confined to the vertical plane. As in Fig. 2, a mass m is attached at the right side of the beam and a mass M is attached at the center. It is noted that m is corresponding to the rotor of the electromagnet, M is corresponding to the rotor of the motor, and the beam is corresponding to the shaft (see Fig. 1). In this configuration, we intend to emphasize the first vibrational mode of the flexible beam. An U-shaped electromagnet is located as an actuator at the right side. As a gap sensor, a standard induction probe of eddy-current type is placed at the same position in the right side of the beam. Parameters of this experimental apparatus are given in Table 1. The beam weight, including m and M, is supported by having a steady-state current I (or, a steady-state voltage E). Stabilization of the system can be accomplished by controlling the corresponding voltage perturbation e.

2.2. Model Formulation

Several approaches can be considered to obtain its mathematical model; e.g., a purely analytic approach which results in complex distributed-parameter systems represented by partial differential equations, or a finite-element approach with the assistance of computer programs which usually generates high-order finite-dimensional systems represented by ordinally differential equations. Among them, the approach taken here may be the simplest one. In the following, the beam is described by a simple multi-mass linear system. Due to the structure of the apparatus, we will include up to the first vibrational mode of the beam, as well as the rigid body motion, in the model. There is no need to say that, if necessary, we can build a more precise mathematical model using the approach mentioned above.

We assume that a half of the mass of the beam can be included into M, and a quarter of it can be included into m. Under these assumptions, we will consider the dynamical equations for m and M, respectively. This naturally leads to a simple lumped-parameter model of the beam, in which the effect of the first vibrational mode is taken into account. Let X_1 be the steady-state gap between the electromagnet and the beam at the position of m, X_2 be the steady-state deflection of the beam from the base line at the position of M, I be the coil current in the steady-state, and E be the corresponding voltage. Further, let the small perturbations of the above quantities be x_1, x_2, i, and e, respectively (see Fig. 2). Then the following equations of motions can be obtained.

$$m\frac{d^2x_1}{dt^2} = mg-k\left(\frac{I+i}{X_1+x_1}\right)^2+\alpha[2(X_2+x_2)-x_1] +\beta\frac{d}{dt}[2(X_2+x_2)-x_1] \quad (1)$$

$$M\frac{d^2x_2}{dt^2} = Mg-2\alpha[2(X_2+x_2)-x_1] -2\beta\frac{d}{dt}[2(X_2+x_2)-x_1]. \quad (2)$$

The second term in the right-hand side of (1) represents the attractive force of the electromagnet and k, which will be determined by experimental data, denotes the corresponding coefficient. Both the third and the fourth terms in the right-hand side of (1) represent the restoring force generated by the deflection of the beam. The coefficients α and β will be also determined by experimentally obtained data. While, both the second and the third terms in the right-hand side of (2) represent the reaction of the above stated force.

Although these equations are nonliner, as is well known, we can easily obtain the linearized equations for the small perturbations around the steady-state points. In the steady-state, we have

$$0 = mg-k\left(\frac{I}{X_1}\right)^2+2\alpha X_2, \quad 0 = Mg-4\alpha X_2. \quad (3)$$

From this, the linearized equations are

$$m\frac{d^2x_1}{dt^2} = \left(\frac{M+2m}{X_1}g-\alpha\right)x_1+2\alpha x_2 -\frac{(M+2m)g}{I}\,i-\beta\frac{dx_1}{dt}+2\beta\frac{dx_2}{dt} \quad (4)$$

$$M\frac{d^2x_2}{dt^2} = 2\alpha x_1-4\alpha x_2+2\beta\frac{dx_1}{dt}-4\beta\frac{dx_2}{dt}. \quad (5)$$

For the relationship between the applied voltage e and the coil current i, the equation can be

$$Ri+L\frac{di}{dt} = e \quad (6)$$

where R and L denote the resistance and the inductance of the electromagnet, respectively. The values of R and L have been determined by experiments.

The sensor provides us with the information for the gap x_1. Hence the measurement equation is

$$y_g = x_1. \quad (7)$$

Now, from experimentally obtained data, we can determine the following values; k = 0.0034 $\mathrm{Nm^2/A^2}$, α = 2064 N/m, and β = 0.327 Ns/m. Thus, summing up the results, the state equations for the magnetic suspension system are

$$\dot{x}_g = A_gx_g+B_gu_g, \quad y_g = C_gx_g \quad (8)$$

where $x_g := [x_1\ x_2\ \dot{x}_1\ \dot{x}_2\ i]^T$, $u_g := e$ and

$$A_g=\begin{bmatrix} 0.0 & 0.0 & 1.0 & 0.0 & 0.0 \\ 0.0 & 0.0 & 0.0 & 1.0 & 0.0 \\ 7070 & 712 & -0.327 & 0.654 & -41.9 \\ 399 & -797 & 0.654 & -1.31 & 0.0 \\ 0.0 & 0.0 & 0.0 & 0.0 & -18.0 \end{bmatrix} \quad (9a)$$

$$B_g=\begin{bmatrix} 0.0 \\ 0.0 \\ 0.0 \\ 0.0 \\ 0.317 \end{bmatrix} \qquad C_g=\begin{bmatrix} 1 & 0 & 0 & 0 & 0 \end{bmatrix} \quad (9b)$$

with (A_g, B_g) controllable, and (A_g, C_g) observable. The transfer function of this system is

$$G(s) = \frac{-13.3}{(s+18.0)(s+84.4)(s-84.1)} \times\frac{(s+0.654-j28.2)(s+0.654+j28.2)}{(s+0.697-j28.8)(s+0.697+j28.8)}. \quad (10)$$

For the magnetic suspension system described above, our principal objective is stabilization. Further, the system should be stabilized robustly against the followings; i.e., the unmodeled higher order vibrational dynamics of the beam, the neglected higher order terms in the Taylor series expansions in the linearization procedure, the parameter errors in the beam and in the electromagnet such as k, α, β, m, M, R and L, the effect of the eddy-current in the electromagnet, and so on. To this end, we will use the H^∞ control theory in the next section.

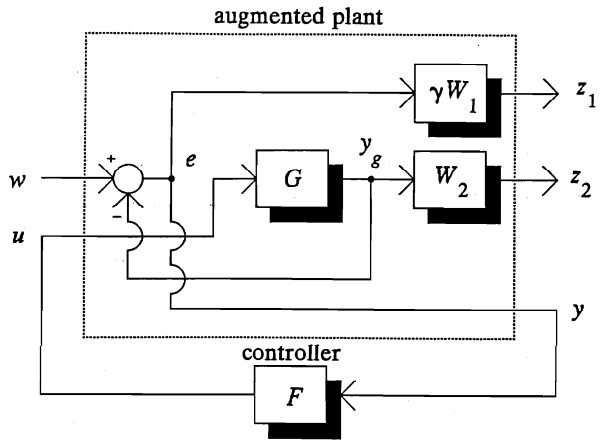

Fig. 3. Plant augmentation.

3. Controller Design

3.1. Mixed Sensitivity Problem

Consider the system shown in Fig. 3. Let us focus our attention on the transfer function from w to e, called the sensitivity function $S(s)$, and the transfer function from w to y_g, called the complementary sensitivity function $T(s)$. The sensitivity function $S(s)$ and the complementary sensitivity function $T(s)$ are defined as

$$S(s) := (I+L(s))^{-1} \tag{11}$$

$$T(s) := L(s)(I+L(s))^{-1} = I-S(s) \tag{12}$$

where $L(s) := G(s)F(s)$ denotes the loop transfer function. It is well known that these functions play an important role in robust feedback control system design. In the following, $\overline{\sigma}(\cdot)$ denotes the greatest singular value of a matrix, and the H^∞-norm is defined as

$$\| \Phi(s) \|_\infty := \sup_\omega \overline{\sigma}(\Phi(j\omega)) \tag{13}$$

for a proper stable transfer function $\Phi(s)$.

Firstly, it is known that the requirement for disturbance attenuation in the feedback system can be specified with the sensitivity function $S(s)$ as

$$\overline{\sigma}(S(j\omega)) < | \gamma^{-1} W_1^{-1}(j\omega) | \quad \text{for all } \omega. \tag{14}$$

In (14), $W_1(s)$ is a desired frequency weighting factor whose gain is relatively large in a low frequency range and $\gamma > 0$ is an adjusting scalar parameter. It is easy to see that the disturbance attenuation requirement (14) can be rewritten as

$$\| \gamma W_1(s) S(s) \|_\infty < 1. \tag{15}$$

Secondly, let us consider robust stability of the feedback system in terms of the complementary sensitivity function $T(s)$. Suppose that the plant $G(s)$ is perturbed as

$$G'(s) = (I+\Delta(s))G(s) \tag{16}$$

where $\Delta(s)$ denotes multiplicative plant perturbations. We will assume that $G'(s)$ has the same number of unstable modes as $G(s)$, and that the nominal feedback system is stable. Then, if

$$\overline{\sigma}(T(j\omega)) < | W_2^{-1}(j\omega) | \quad \text{for all } \omega \tag{17}$$

the system remains stable for all $\Delta(s)$ satisfying

$$\overline{\sigma}(\Delta(j\omega)) \leq | W_2(j\omega) | \quad \text{for all } \omega. \tag{18}$$

Hence, as the robust stability condition, we have

$$\| W_2(s) T(s) \|_\infty < 1. \tag{19}$$

The frequency weighting factor $W_2(s)$ is usually small at low frequencies and increases its magnitude at higher frequencies.

The design specifications as in (15) and (19) can be combined into a single H^∞-norm specification

$$\left\| \begin{matrix} \gamma W_1(s) S(s) \\ W_2(s) T(s) \end{matrix} \right\|_\infty < 1 \tag{20}$$

where we have used the following matrix inequality

$$\frac{1}{\sqrt{2}} \overline{\sigma}\left(\begin{bmatrix} A \\ B \end{bmatrix} \right) \leq \max \{ \overline{\sigma}(A), \overline{\sigma}(B) \} \leq \overline{\sigma}\left(\begin{bmatrix} A \\ B \end{bmatrix} \right). \tag{21}$$

This ensures that the requirements (15) and (19) are reasonably approximated (within 3 dB). Now the mixed sensitivity problem is to find a controller $F(s)$ such that the system is internally stable and the specification (20) is satisfied.

3.2. H^∞ Design

In this study, the weighting functions $W_1(s)$ and $W_2(s)$ are chosen as

$$W_1(s) = \frac{1.3298}{1+s/(2\pi \cdot 0.016)} \tag{22}$$

$$W_2(s) = 10^{-4} \left(1+\frac{s}{2\pi \cdot 0.002} \right) \times \left(1+\frac{s}{2\pi \cdot 160} \right) \left(1+\frac{s}{2\pi \cdot 200} \right). \tag{23}$$

While the value of γ will be increased according to the design iterations until the specification (20) can be no longer satisfied (γ-iteration).

Table 2. State-space realization of augmented plant.

$$A=\begin{bmatrix} 0.00 & 0.00 & 1.00 & 0.00 & 0.00 & 0.00 \\ 0.00 & 0.00 & 0.00 & 1.00 & 0.00 & 0.00 \\ 7.07\times10^{3} & 7.12\times10^{2} & -3.27\times10^{-1} & 6.54\times10^{-1} & -4.19\times10 & 0.00 \\ 3.99\times10^{2} & -7.97\times10^{2} & 6.54\times10^{-1} & -1.31 & 0.00 & 0.00 \\ 0.00 & 0.00 & 0.00 & 0.00 & -1.80\times10 & 0.00 \\ -1.00 & 0.00 & 0.00 & 0.00 & 0.00 & -1.01\times10^{-1} \end{bmatrix}, \quad [B_1 \;\; B_2]=\begin{bmatrix} 0.00 & 0.00 \\ 0.00 & 0.00 \\ 0.00 & 0.00 \\ 0.00 & 0.00 \\ 0.00 & 3.17\times10^{-1} \\ 1.00 & 0.00 \end{bmatrix}$$

$$\begin{bmatrix} C_1 \\ C_2 \end{bmatrix}=\begin{bmatrix} 0.00 & 0.00 & 0.00 & 0.00 & 0.00 & 2.30 \\ 1.01\times10^{-1} & 1.01\times10^{-2} & 7.99\times10^{-3} & 1.38\times10^{-5} & -5.92\times10^{-4} & 0.00 \\ -1.00 & 0.00 & 0.00 & 0.00 & 0.00 & 0.00 \end{bmatrix}, \quad \begin{bmatrix} D_{11} & D_{12} \\ D_{21} & D_{21} \end{bmatrix}=\begin{bmatrix} 0.00 & 0.00 \\ 0.00 & -8.35\times10^{-8} \\ 1.00 & 0.00 \end{bmatrix}$$

Table 3. State-space realization of controller.

$$A_f=\begin{bmatrix} -2.98\times10^{3} & -1.40 & -3.49 & -1.29\times10^{-3} & 8.27\times10^{-2} & 3.06\times10^{4} \\ -1.69\times10^{2} & -7.97\times10^{-2} & -2.55\times10^{-1} & 1.00 & 4.69\times10^{-3} & 1.73\times10^{3} \\ -2.44\times10^{5} & 5.94\times10^{2} & -3.78\times10^{2} & 5.45\times10^{-1} & -3.49\times10 & 2.57\times10^{6} \\ -1.38\times10^{4} & -8.04\times10^{2} & -2.08\times10 & -1.31 & 3.95\times10^{-1} & 1.46\times10^{5} \\ 3.02\times10^{7} & 5.47\times10^{4} & 8.25\times10^{4} & 6.73\times10 & -3.22\times10^{3} & -3.56\times10^{8} \\ 0.00 & 0.00 & 0.00 & 0.00 & 0.00 & -1.01\times10^{-1} \end{bmatrix}$$

$$B_f=\begin{bmatrix} -4.20\times10^{2} & -2.39\times10 & -3.54\times10^{4} & -2.01\times10^{3} & 0.00 & 1.00 \end{bmatrix}^T$$

$$C_f=\begin{bmatrix} 9.54\times10^{7} & 1.73\times10^{5} & 2.61\times10^{5} & 2.12\times10^{2} & -1.01\times10^{4} & -1.12\times10^{9} \end{bmatrix}$$

Recall that the open-loop plant $G(s)$ has three more poles than zeros. Hence we need at least -60 dB/decade roll-off for the complementary sensitivity, which is the same as the open-loop plant. As a result, $W_2(s)$ becomes an improper function as in (23). But this ensures that the direct feedthrough matrix D_{12} in (24) has full rank (see Table 2) and the resulting controller is proper. The frequency weighting $W_2(s)$ has been determined so that the closed-loop system possesses sufficient robust stability against uncertainties such as the unmodeled higher order vibrational dynamics. Subject to these constraints, we try to minimize the weighted sensitivity $W_1(s)S(s)$ as much as possible using γ-iteration.

With the weighting functions $\gamma W_1(s)$ and $W_2(s)$, let us form an augmented plant as shown in Fig. 3. A few hand calculations enable us to obtain the state-space realization of the augmented plant as follows (see Table 2)

$$\dot{x} = Ax+B_1w+B_2u \tag{24a}$$

$$z = C_1x+D_{11}w+D_{12}u \tag{24b}$$

$$y = C_2x+D_{21}w+D_{22}u \tag{24c}$$

where we have chosen $\gamma = 17.2$. It is noted that the maximal value of γ for which (20) holds, is 21.0. These H^∞ designs have been carried out using the iterative computing environment MATLAB [13].

The obtained H^∞ "central" controller [10],[11] is

$$F(s) = C_f(sI-A_f)^{-1}B_f$$

$$= \frac{-5.05\times10^{10}(s+1.972)(s+18.0)(s+84.4)}{(s+0.101)(s+1176-j401)(s+1176+j401)(s+4232)} \times\frac{(s+0.697-j28.8)(s+0.697+j28.8)}{(s+0.654-j28.2)(s+0.654+j28.2)} \tag{25}$$

(see Table 3). This controller has six state variables, which is the same as the augmented plant, is stable and is strictly proper.

The Bode plots of the sensitivity S with $\gamma^{-1}W_1^{-1}$, and the complementary sensitivity T with W_2^{-1} are shown in Fig. 4 and Fig. 5, respectively. As in Fig. 4 and 5, the sensitivity S approaches to $\gamma^{-1}W_1^{-1}$ at low frequencies, and the complementary sensitivity T approaches to W_2^{-1} at high frequencies. These are essentially based on the remarkable all-pass property in the H^∞ theory. Thus the H^∞ theory provides a direct method for achieving a loop-shaping in the frequency domain. In Fig. 6, the Bode plots of the loop transfer function are shown. At low frequencies, the loop transfer function has a large gain. An increasing phase-lead can be seen in the middle frequency range, which shows the gain margin of 22.5 dB and the phase margin of 26 degrees. The cross-over frequency is about 9 Hz and the desirable roll-off property can be seen at high frequencies.

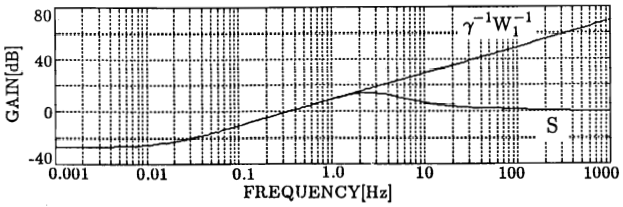

Fig. 4. Sensitivity function.

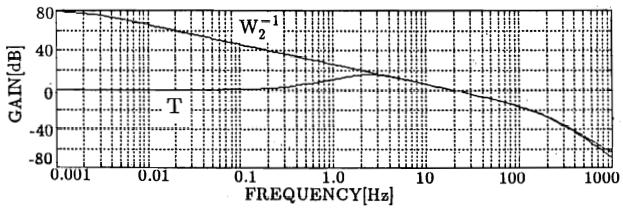

Fig. 5. Complementary sensitivity function.

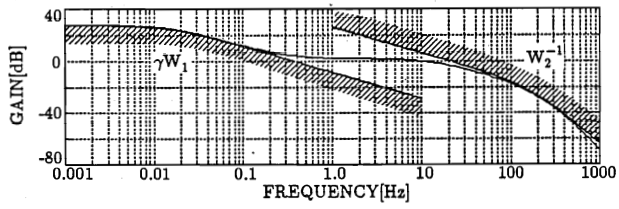

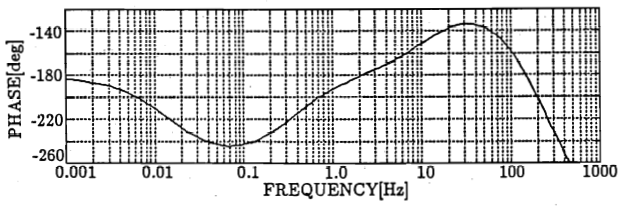

Fig. 6. Loop transfer function.

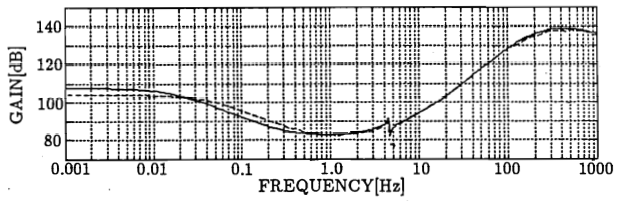

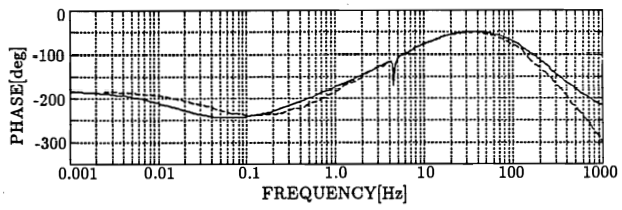

Fig. 7. Controller.

4. Implementation and Experimental Results

4.1. Implementation of Digital Controller

The obtained continuous-time controller (25) is discretized via the popular Tustin transform

$$s = \frac{2}{T}\frac{z-1}{z+1} \tag{26}$$

at the sampling rate of 40 μs. The Bode plots of the controller are given in Fig. 7. The solid line in the figure shows the ideal continuous-time controller and the broken line shows the discretized controller with the transformation (26).

The structure of the digital signal processor (DSP)-based controller is shown in Fig. 8. Real-time control is accomplished via the processor NEC μPD77230 on a special board, which can execute one instruction in 150 ns with 32-bit floating point arithmetic. The control algorithm is written in the assembly language for the DSP and the software development is assisted by the host personal computer NEC PC9801. The data acquisition boards consist of a 12-bit A/D converter module DATEL ADC-B500 with the maximum conversion speed of 0.8 μs and a 12-bit D/A converter DATEL DAC-HK12 with the maximum conversion speed of 3 μs.

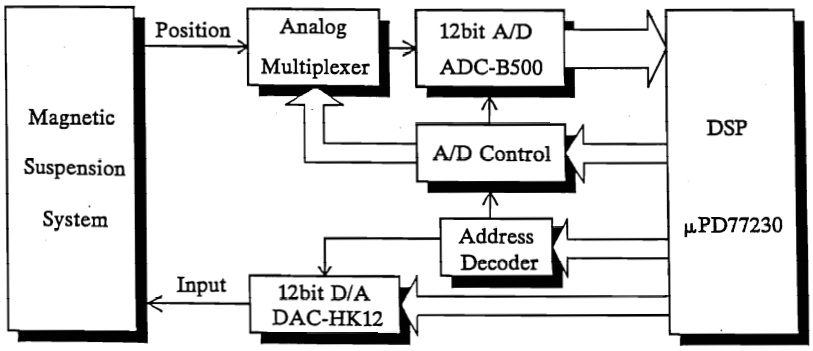

Fig. 8. DSP-based controller.

4.2. Experimental Results

We first evaluate the nominal stability of the designed control system with time-responses for a step-type disturbance. The disturbance is added as an applied voltage in the electromagnet, which in fact amounts to about 20 % of the steady-state force. Fig. 9 shows the displacements of x_1 and x_2. From this result, we can see that the nominal stabilization of the system is achieved. In Fig. 10, the stiffness at the position of the electromagnet is also shown. From these data, we can see that high stiffness has been achieved at low frequencies. Further, it should be noted that the stiffness is not necessarily deteriorated near the resonance frequencies. This implies that the system is well stabilized.

Since our concerns are also in robust stability against various model uncertainties, we further continue the same experiments with the plant parameters changed. The parameters have changed in the following ways;

(i) m = 6.95 kg, which amounts to a 20 % increase for the nominal value of 5.8 kg,

(ii) M = 12.31 kg, which amounts to a 20 % increase for the nominal value of 10.36 kg,

(iii) R = 61.7 Ω, which amounts to a 10 % increase for the nominal value of 57.0 Ω.

The results are shown in Fig. 11 - 13. In any case it can be seen that the beam is still suspended stably by the controlled magnetical forces. Therefore, these experimental results confirm us that the designed magnetic suspension system is robustly stable against various parameter changes.

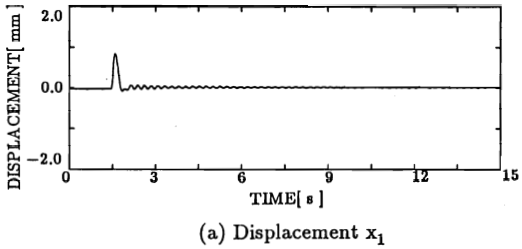

(a) Displacement x_1

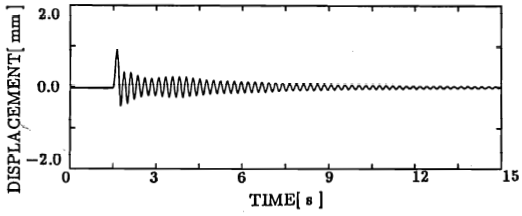

(b) Displacement x_2

Fig. 9. Responses for step-type disturbance (nominal).

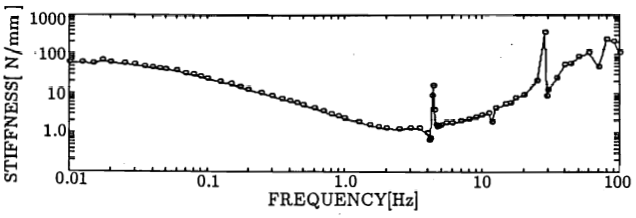

Fig. 10. Stiffness.

5. Conclusions

In this paper, an H^∞ robust control design for a magnetic suspension system with a flexible beam has been presented. Several experimental results showed that the designed magnetic suspension system is robustly stable against various plant perturbations. For the related experimental studies of the H^∞ control, see [14],[15].

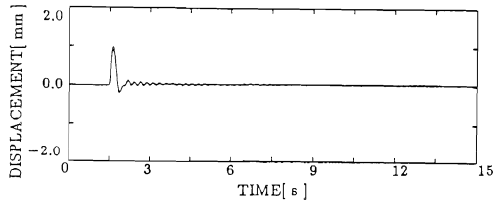

(a) Displacement x_1

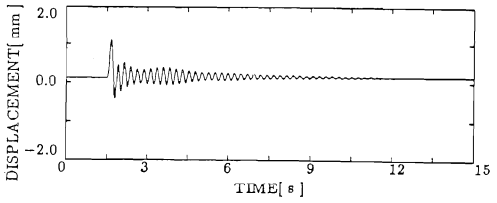

(b) Displacement x_2

Fig. 11. Responses for step-type disturbance (m = 6.95 kg).

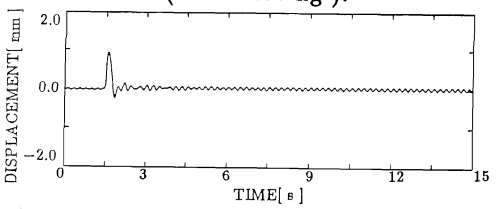

(a) Displacement x_1

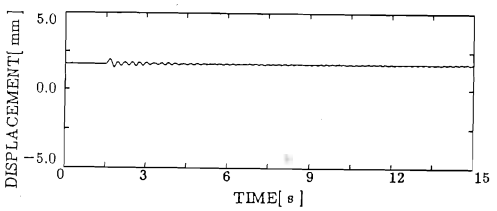

(b) Displacement x_2

Fig. 12. Responses for step-type disturbance (M = 12.31 kg).

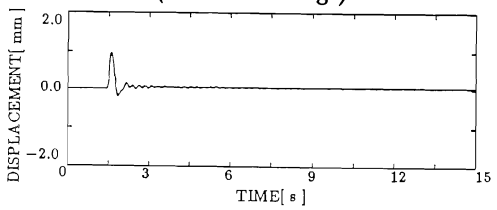

(a) Displacement x_1

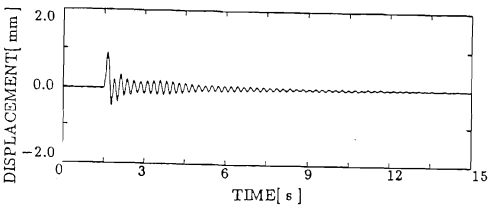

(b) Displacement x_2

Fig. 13. Responses for step-type disturbance (R = 61.7 Ω).

References

[1] G. Schweitzer, Ed., *Magnetic Bearings: Proc. First Int. Symp. Magnetic Bearings.* Berlin: Springer-Verlag, 1989.

[2] F. Matsumura, H. Kobayashi, and Y. Akiyama, "Fundamental equation of horizontal shaft magnetic bearing and its control system design (in Japanese)," *Trans. IEE of Japan*, vol. **101-C**, pp. 137-144, 1981.

[3] F. Matsumura and T. Yoshimoto, "System modeling and control design of a horizontal-shaft magnetic-bearing system," *IEEE Trans. Magnetics*, vol. **MAG-22**, pp. 196-203, 1986.

[4] F. Matsumura, M. Fujita, A. Higashide, and C. Oida, "Stabilizing control of magnetic bearing combining radial control and thrust control using the In-the-Region pole allocation method (in Japanese)," *Trans. IEE of Japan*, vol. **107-D**, pp. 35-41, 1987.

[5] F. Matsumura, M. Fujita, and C. Oida, "Theory and experiment of magnetic bearing combining radial control and thrust control," *IEEE Trans. Magnetics*, vol. **MAG-23**, pp. 2581-2583, 1987.

[6] F. Matsumura, M. Fujita, C. Oida, and A. Higashide, "A damping control for the vibration in a magnetic bearing using the selective turn-over method (in Japanese)," *Trans. IEE of Japan*, vol. **108-C**, pp. 47-54, 1988.

[7] F. Matsumura, M. Fujita, and K. Okawa, "Modeling and control of magnetic bearing systems achieving a rotation around the axis of inertia," to be presented at the *2nd Int. Symp. Magnetic Bearings*, Tokyo, Japan, July 12-14, 1990.

[8] F. Matsumura, M. Fujita, and H. Takahashi, "An observer-based robust stabilization of 3-axes controlled type magnetic bearings using a digital signal processor," to be presented at the *11th IFAC World Congress*, Tallinn, USSR, Aug. 13-17, 1990.

[9] F. Matsumura, M. Fujita, Y. Ozaki, and M. Shimizu, "Stabilization for flexible beam system controlled by magnetic suspension," in *Proc. 11th Int. Conf. Magnetically Levitated Systems and Linear Drives*, Yokohama, Japan, July 7-11, 1989.

[10] K. Glover and J.C. Doyle, "State-space formulae for all stabilizing controllers that satisfy an H_∞-norm bound and relations to risk sensitivity", *Syst. Contr. Lett.*, vol. **11**, pp. 167-172, 1988.

[11] J.C. Doyle, K. Glover, P.P. Khargonekar, and B.A. Francis, "State-space solutions to standard H_2 and H_∞ control problems," *IEEE Trans. Automat. Contr.*, vol. **AC-34**, pp. 831-847, 1989.

[12] K. Uchida and M. Fujita, H^∞ control theory and game theory (in Japanese)," *J. SICE*, vol. **29**, pp. 136-141, 1990.

[13] R.Y. Chiang and M.G. Safonov, *Robust-Control Toolbox User's Guide.* The Math Works, Inc., 1988.

[14] F. Matsumura, M. Fujita, and M. Shimizu, "Robust stabilization of a magnetic suspension system using H^∞ control theory (in Japanese)," *Trans. IEE of Japan*, 1990, submitted for publication.

[15] M. Fujita and F. Matsumura, "H^∞ control of a magnetic suspension system (in Japanese)," *J. IEE of Japan*, 1990, to be published.